

# Cell Surface Markers of Functional Phenotypic Corneal Endothelial Cells

Naoki Okumura,<sup>1,2</sup> Hiroatsu Hirano,<sup>1</sup> Ryohei Numata,<sup>1</sup> Makiko Nakahara,<sup>1</sup> Morio Ueno,<sup>2</sup> Junji Hamuro,<sup>2</sup> Shigeru Kinoshita,<sup>2</sup> and Noriko Koizumi<sup>1</sup>

<sup>1</sup>Department of Biomedical Engineering, Faculty of Life and Medical Sciences, Doshisha University, Kyotanabe, Japan

<sup>2</sup>Department of Ophthalmology, Kyoto Prefectural University of Medicine, Kyoto, Japan

Correspondence: Noriko Koizumi, Department of Biomedical Engineering, Faculty of Life and Medical Sciences, Doshisha University, Kyotanabe 610-0321, Japan; [nkoizumi@mail.doshisha.ac.jp](mailto:nkoizumi@mail.doshisha.ac.jp).

Submitted: June 8, 2014

Accepted: October 24, 2014

Citation: Okumura N, Hirano H, Numata R, et al. Cell surface markers of functional phenotypic corneal endothelial cells. *Invest Ophthalmol Vis Sci*. 2014;55:7610-7618. DOI: 10.1167/iovs.14-14980

**PURPOSE.** Cultured human corneal endothelial cells (HCECs) are anticipated to serve as an alternative to donor corneas for the treatment of corneal endothelial dysfunction. However, corneal endothelial cells (CECs) tend to exhibit fibroblastic transformation, thereby losing their functional phenotype when cultured. The purpose of this study was to investigate the usefulness of surface markers of CECs displaying fibroblastic phenotypes as a means of cell characterization.

**METHODS.** The expression levels of 242 cell surface antigens were screened in cultured human and monkey CECs using flow cytometry. An expression intensity ratio of nonfibroblastic/fibroblastic CECs > 2 and of fibroblastic/nonfibroblastic CECs > 2 were selected as indicating nonfibroblastic and fibroblastic markers, respectively. Nonfibroblastic and fibroblastic CECs were mixed, and CD73-positive and -negative cells were sorted using flow cytometry and further cultured. The functional phenotype of the sorted cells was evaluated according to morphology and the expression of function-related (Na<sup>+</sup>/K<sup>+</sup>-ATPase and ZO-1) and fibroblastic (type I collagen and fibronectin) markers.

**RESULTS.** Flow cytometry analysis demonstrated that CD98, CD166, and CD340 are elevated in HCECs of nonfibroblastic phenotype, while CD9, CD49e, CD44, and CD73 are markers of fibroblastic phenotype HCECs. The CECs that sorted as CD73-negative exhibited normal hexagonal morphology and expressed functional markers, whereas CECs that sorted as CD73-positive exhibited the fibroblastic phenotype.

**CONCLUSIONS.** These markers will be useful for quality control to characterize the phenotype of cells destined for tissue engineering-based therapy. In addition, this selection protocol will provide a novel method for purification of functional cells.

**Keywords:** corneal endothelial cells, cell surface marker, tissue engineering, regenerative medicine

The corneal endothelium regulates the aqueous humor flow to the corneal stroma through a combination of pumps and a leaky barrier function, thereby maintaining corneal transparency.<sup>1</sup> Corneal endothelial cells (CECs) have severely limited proliferative ability,<sup>2,3</sup> so healing of wounds to the corneal endothelium is mainly performed by cell migration and spreading. Consequently, severe damage to the corneal endothelium resulting from pathologic conditions, such as Fuchs' corneal endothelial dystrophy, surgical stress, or endotheliitis, leads to corneal endothelial dysfunction, and ultimately to the loss of corneal transparency.<sup>4-6</sup> Corneal transplantation is the only therapeutic choice for treating corneal endothelial dysfunction, but this procedure is fraught with several associated problems, including a worldwide shortage of donor corneas and the technical difficulty of the surgical procedure itself, especially for patients with aphakia, postfiltration surgery, and post-tube surgery for glaucoma.<sup>5,7</sup>

Tissue engineering presently is viewed as a potential protocol that may overcome these problems and provide alternative treatments for corneal endothelial dysfunction.<sup>5,8</sup> Indeed, transplantation of cultured corneal endothelium as a form of sheet, with or without carrier, has enabled the recovery

of corneal transparency in animal models.<sup>9-12</sup> However, cultured corneal endothelial sheets, as cell monolayers, are highly fragile, making transplantation into the anterior chamber technically difficult. Consequently, researchers, including our group, are investigating the possibility of transplantation of cultured cells in the form of a cell suspension.<sup>13-16</sup> For instance, we reported that injection of cultured CECs, in combination with a Rho kinase (ROCK) inhibitor, enables regeneration of the corneal endothelium in rabbit and monkey models.<sup>16</sup>

Cultured human CECs (HCECs) have been anticipated as an alternative tissue source to donor corneas, but the in vitro expansion of HCECs is a bottleneck that currently limits therapy based on tissue engineering. The technical obstacles to cell cultivation arise from a number of features distinct to HCECs; namely, their limited proliferative ability and tendency to undergo spontaneous fibroblastic changes under culture conditions. These obstacles have persisted despite attempts to develop culture methods specifically for clinical use.<sup>17-21</sup>

We previously reported the usefulness of a ROCK inhibitor in enhancing cell proliferation through activation of the PI3 kinase/Akt signaling pathway.<sup>17,22</sup> The use of a conditioned

medium obtained from GMP-grade human bone marrow-derived mesenchymal stem cells (MSCs) also can potentiate HCEC proliferation.<sup>20</sup> We investigated methods to circumvent fibroblast formation by studying the fibrosis-related signaling pathways and found that activation of the TGF- $\beta$  signaling pathway has an important role in fibroblastic differentiation. This finding led to the development of a culture protocol for clinical application using SB431542 to inactivate TGF- $\beta$  signaling, which suppressed fibroblastic changes and maintained functional phenotypes.<sup>21</sup> This recent progress has reinvigorated the investigation of protocols for culturing of HCECs for clinical use.

In the present study, we screened the surface markers of HCECs showing normal (nonfibroblastic) and fibroblastic phenotypes as a quality control measure for the production of cultured HCECs for clinical use. We demonstrated that CD98, CD166, and CD340 are dominantly expressed in the normal CEC phenotype, while CD9, CD44, CD49e, and CD73 are markers for fibroblasts. In addition, CECs expressing a fibroblastic marker (e.g., CD73) showed increased expression of epithelial mesenchymal transformation (EMT) inducer genes, a fibroblastic phenotype based on morphological changes, and a greater production of extracellular matrix, in addition to the loss of the functional phenotype.

## MATERIALS AND METHODS

### Ethics Statement

The human tissue used in this study was handled in accordance with the tenets set forth in the Declaration of Helsinki. Human donor corneas were obtained from SightLife (Seattle, WA, USA). Informed written consent for eye donation for research was obtained from the next of kin of all deceased donors. All tissues were recovered under the tenets of the Uniform Anatomical Gift Act (UAGA) of the particular state in which the donor consent was obtained and the tissue was recovered. The monkey corneas used in this study were handled in accordance with the ARVO Statement for the Use of Animals in Ophthalmic and Vision Research. The protocols for the general welfare of the animals from which the corneas were harvested and the procedures for isolation of the corneas were approved by the institutional animal care and use committee of Nissei Bilis Co., Ltd. (Otsu, Japan). The animals were euthanized with an overdose of intravenous pentobarbital sodium for other research purposes, according to the guidelines on euthanasia of the American Veterinary Medical Association (AVMA); corneas were harvested after confirmation of cardiopulmonary arrest by veterinarians provided by Nissei Bilis Co., Ltd.

### Cell Cultures of HCECs

Human corneas were stored at 4°C in storage medium (Optisol-GS; Chiron Vision, Irvine, CA, USA). The HCECs were cultured according to published protocols, with some modifications.<sup>21</sup> A total of 10 human donor corneas (>60 years old) was used for the experiments. Briefly, the Descemet's membranes with the CECs were stripped from donor corneas and digested at 37°C with 1 mg/mL collagenase A (Roche Applied Science, Penzberg, Germany) for 12 hours. The HCECs obtained from a single donor cornea were seeded in one well of a 48-well plate coated with FNC Coating Mix (Athena Environmental Sciences, Inc., Baltimore, MD, USA). The culture medium was prepared according to published protocols. Briefly, basal medium was prepared with OptiMEM-I (Life Technologies Corp., Carlsbad, CA, USA), 8% fetal bovine serum (FBS), 5 ng/mL epidermal growth factor (EGF; Sigma-Aldrich Corp., St. Louis, MO, USA),

20  $\mu$ g/mL ascorbic acid (Sigma-Aldrich Corp.), 200 mg/L calcium chloride (Sigma-Aldrich Corp.), 0.08% chondroitin sulfate (Wako Pure Chemical Industries, Ltd., Osaka, Japan), and 50  $\mu$ g/mL of gentamicin. Inactivated 3T3 fibroblasts, prepared as previously described,<sup>20</sup> then were cultured with basal medium for 24 hours, and the conditioned basal medium was recovered as culture medium for the HCECs. The HCECs were cultured using culture medium prepared as above at 37°C in a humidified atmosphere containing 5% CO<sub>2</sub>, and the culture medium was changed every 2 days. The HCECs were passaged at ratios of 1:2 using 0.05% Trypsin-EDTA for 5 minutes at 37°C when they reached confluence. The HCECs at passages 2 through 5 were used for all experiments.

### Immortalization of HCECs Using Lentiviral Transduction of SV40 Large T Antigen and hTERT Genes

The HCECs exhibiting normal morphology and fibroblastic morphology were immortalized for cell sorting experiments using SV40 and hTERT to produce normal iHCEC and fibroblastic iHCECs cell lines, respectively. The coding sequences of the SV40 large T antigen and hTERT genes were amplified through PCR and were TA-cloned into a commercial lentiviral vector. The lentiviral vectors then were transfected to 293T cells (RCB2202; Riken Bioresource Center, Ibaraki, Japan), along with three helper plasmids (pLP1, pLP2, and pLP/VSVG; Life Technologies Corp.), using a commercial transfection reagent (Fugene HD; Promega Corp., Madison, WI, USA) for 48 hours. The supernatant of the culture medium was harvested, centrifuged briefly, and stored in a freezer at -80°C. For lentiviral transduction, the virus-containing supernatants of both genes were added to the cultures of HCECs in the presence of 5  $\mu$ g/mL of polybrene. The immortalized cells were cultured in Dulbecco's modified Eagle's medium (DMEM; Life Technologies Corp.) containing 10% FBS, and 1% penicillin and streptomycin; the medium was changed every two days. Once the immortalized cells were 80% confluent, the cells were trypsinized with 0.05% trypsin-EDTA and passaged.

### Cell Culture of Monkey CECs (MCECs)

The MCECs were cultured as described previously.<sup>12</sup> Briefly, the Descemet's membrane including the MCECs was stripped and digested at 37°C for 2 hours with 1 mg/mL collagenase A. The resulting cells were suspended in culture medium, then seeded in 1 well of a 6-well plate coated with FNC Coating Mix. The MCECs were cultured at 37°C in a medium composed of DMEM supplemented with 10% FBS, 50 U/mL penicillin, 50  $\mu$ g/mL streptomycin, and 2 ng/mL FGF-2 (Life Technologies Corp.) in a humidified atmosphere containing 5% CO<sub>2</sub>. The culture medium was changed every 2 days and MCECs were passaged at ratios of 1:2 to 4 using 0.05% Trypsin-EDTA (Life Technologies Corp.). Cultivated MCECs at passages 2 through 5 were used for all experiments.

### Flow Cytometry

Screening of cell surface markers was conducted by assessing the expression of markers through the Human Cell Surface Marker Screening Panel (BD Biosciences, San Jose, CA, USA) according to the manufacturer's protocol. Briefly, cultured HCECs (of normal morphology and fibroblastic morphology; not immortalized cells) and cultured MCECs (normal morphology and fibroblastic morphology) were detached with Accutase (BD Biosciences) at 37°C, washed twice with PBS, passed through a BD Falcon 70  $\mu$ m cell strainer (BD Biosciences), incubated in OptiMEM-I with the addition of 100 units/mL

DNase for 15 minutes at room temperature, and resuspended with BD Pharmingen Stain Buffer (BD Biosciences) containing 5 mM EDTA. The HCECs or MCECs ( $1.0 \times 10^4$  cells, respectively) were incubated with primary 242 antibodies and isotype IgGs (BD Biosciences) at the dilution indicated by the manufacturer's protocol for 30 minutes on ice. The cells were washed with BD Pharmingen Stain Buffer containing 5 mM EDTA and then incubated with AlexaFluor 647 conjugated IgGs (1:200 dilution, BD Biosciences) for 30 minutes. The cells were washed again with BD Pharmingen Stain Buffer containing 5 mM EDTA and analyzed by flow cytometry using a BD FACSCant II instrument (BD Biosciences) and CellQuest Pro software (BD Biosciences). For cell sorting experiments, MCECs or immortalized HCECs were washed twice with PBS and incubated with Accumax (Innovative Cell Technologies, San Diego, CA, USA) for 10 minutes at 37°C before cell sorting. Cells were recovered in FACS buffer composed of DMEM without Phenol Red (Nacalai Tesque, Kyoto, Japan) + 2% FBS, passed through a BD Falcon 70  $\mu$ m cell strainer (BD Biosciences), and resuspended in FACS buffer. The cells then were incubated with antibodies (CD73, 1:300; BD Pharmingen Stain Buffer), and mouse IgG (1:62.5; Dako, Glostrup, Denmark) for 30 minutes at 4°C, then incubated with AlexaFluor 488 conjugated IgG (1:1000 dilution; BD Biosciences) for 30 minutes at 4°C. After washing three times with PBS, the cells were resuspended in FACS buffer supplemented with 2  $\mu$ g/mL propidium iodide (Sigma-Aldrich Corp.) at a density of  $5 \times 10^6$  to  $1 \times 10^7$  cells/ml. The CD73-positive and -negative cells were sorted using a BD FACSaria (BD Biosciences) and seeded at a density of  $2.5 \times 10^5$  cells on a 24-well cell culture plate for subsequent analysis.

### Immunofluorescent Staining

The MCECs and HCECs were cultured at a density of  $1 \times 10^5$  cells/well in a 24-well cell culture plate coated with FNC Coating Mix and were maintained for 3 to 4 weeks for immunofluorescence analysis. Cells were fixed in 95% ethanol supplemented with 5% acetic acid for 10 minutes at room temperature and incubated for 30 minutes with 1% BSA. Samples were incubated overnight at 4°C with antibodies against CD73 (1:300; BD Pharmingen Stain Buffer), CD166 (1:300; BD Pharmingen Stain Buffer), ZO-1 (1:300; Zymed Laboratories, South San Francisco, CA, USA), and Na<sup>+</sup>/K<sup>+</sup>-ATPase (1:300; Upstate Biotech, Lake Placid, NY, USA). After washing with PBS, either Alexa Fluor 488-conjugated goat anti-mouse (Life Technologies) or Alexa Fluor 594-conjugated goat anti-rabbit IgG (Life Technologies) was used as the secondary antibody at a 1:1000 dilution. Nuclei were stained with DAPI (Vector Laboratories, Burlingame, CA, USA). The cells, cultured

in a 48-well cell culture plate, were directly examined by fluorescence microscopy (BZ-9000; Keyence, Osaka, Japan).

### Semiquantitative RT-PCR

Total RNA was extracted from MCECs and HCECs using the RNeasy Mini kit (Qiagen, Hilden, Germany), after which the quality of the RNA preparations was measured with a NanoDrop spectrophotometer (Thermo Fisher Scientific, Inc., Waltham, MA, USA). The cDNA was synthesized using ReverTra Ace (Toyobo, Osaka, Japan) and subjected to PCR with the specific primers listed in Table 1. Glyceraldehyde 3-phosphate dehydrogenase (GAPDH) was used as an internal control for gene analysis. The PCR reactions were performed using Extaq DNA polymerase (Takara Bio, Inc., Otsu, Japan) under the following conditions: denaturation at 94°C for 30 seconds, 33 cycles of annealing at 54°C for 30 seconds, and elongation at 72°C for 30 seconds. The PCR products were separated by electrophoresis on 1.5% agarose gels, stained with ethidium bromide, and detected under ultraviolet illumination.

### Quantitative Real-Time PCR

Gene expression levels were analyzed using TaqMan real-time PCR (Applied Biosystems, Foster City, CA, USA). Total RNA was extracted with the RNeasy mini kit, and cDNA was synthesized using ReverTra Ace. Taqman primers for *ZO1*, Hs01551861\_ml; *ATP1A1*, Hs00167556\_ml; *FNI*, Hs01549976\_ml; and TaqMan predevelopment human GAPDH (Applied Biosystems) were used. The PCR was performed using the StepOne (Applied Biosystems) real-time PCR system. The GAPDH was used as an internal standard.

### Statistical Analysis

The statistical significance (*P* value) of mean values for 2-sample comparisons was determined by the Student's *t*-test. The statistical significance for the comparison of multiple sample sets was determined with the Dunnnett's multiple-comparisons test. Values shown on the graphs represent the mean  $\pm$  SE.

## RESULTS

### Cell Surface Markers of Normal and Fibroblastic Morphological CECs

Primate CECs often exhibit morphological fibroblastic changes and lose their functional phenotypes,<sup>21,23</sup> although a cell culture maintaining the normal phenotype sometimes is

TABLE 1. Oligonucleotide Sequences

Gene	Sense Primer	Antisense Primer	Size, bp
<i>CD73</i>	5'-GTTCCCTGTAGTCCAGGCCTATG-3'	5'-ACATTTTCATCCGTGTGTCTCAG-3'	316
<i>CD166</i>	5'-CCCCAGAGGAATTTTGTGTTTAC-3'	5'-AGCCTGATGTTATCTTTCATCCA-3'	289
<i>ZO1</i>	5'-CCAGCTTCTCGAAGAACCAC-3'	5'-GAACGAGGCATCATCCCTAA-3'	218
<i>ATP1A1</i>	5'-ACGGCAGTGATCTAAAGGACAT-3'	5'-GAAGAATCATGTGAGCAGCTTG-3'	255
<i>CDH2</i>	5'-CCAGGTCTTGAGCAGTGACA-3'	5'-TTCCAACCTTCACCTTGACC-3'	185
<i>COL1A1</i>	5'-ATGGATTCAGTTCGAGTATGG-3'	5'-GACAGTGACGCTGTAGGTGAAG-3'	242
<i>COL4A1</i>	5'-AGCAAGGTGTTACAGGATTGGT-3'	5'-AGAAGGACACTGTGGGTCTCT-3'	392
<i>COL8A1</i>	5'-AGAGGGGAGAAAGGACCAATAG-3'	5'-CCTACTTCACCAAGGAAACCTG-3'	221
<i>SNAI1</i>	5'-ACTGCAAATACTGCAACAAGGA-3'	5'-TCTTGACATCTGAGTGGGTCTG-3'	240
<i>SNAI2</i>	5'-CCTGTGCATACCACAACCAGAGA-3'	5'-CTTCATCACTAATGGGGCTTTC-3'	211
<i>ZEB1</i>	5'-TTAGTTGCTCCCTGTGCAGTTA-3'	5'-TGTGTGAGCTATAGGAGCCAGA-3'	261
<i>GAPDH</i>	5'-GAGTCAACGGATTTGGTTCGT-3'	5'-TTGATTTTGGAGGGATCTCG-3'	238

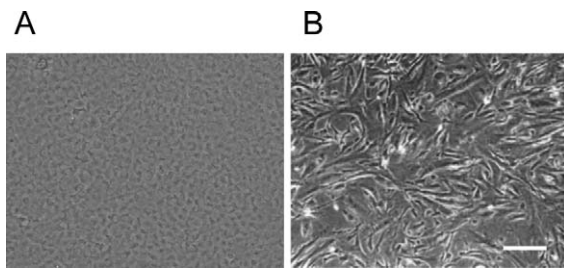


**FIGURE 1.** Nonfibroblastic and fibroblastic phenotypes exhibited during primary culture of HCECs. Primary cultivated HCECs demonstrated various phenotypes during cultivation using the same culture protocol. Representative phenotypes are presented. (A) Nonfibroblastic phenotype in which the cells maintained the characteristic polygonal contact-inhibited shape and monolayer. (B) Fibroblastic phenotype in which the cells were stratified and fibroblastic. Scale bar: 100  $\mu$ m.

observed. Representative phenotypes of primary cultured nonfibroblastic (normal) and fibroblastic cultured HCECs are shown (Figs. 1A, 1B). Cell surface markers for normal morphological CECs and fibroblastic CECs were evaluated by screening for the expression of 242 cell surface antigens by flow cytometry. The ratio of the mean fluorescence intensity of normal CECs and fibroblastic CECs was calculated. The markers that showed ratios of primary cultured nonfibroblastic/fibroblastic HCECs  $> 2$  (Supplemental Table S1) and primary cultured fibroblastic/nonfibroblastic HCECs  $> 2$  (Supplemental Table S2) are listed. The markers conserved in humans and monkeys are more reliable, so we further screened cell surface markers for normal morphological MCECs and fibroblastic MCECs (Fig. 2A), selecting markers that showed nonfibroblastic/fibroblastic or fibroblastic/nonfibroblastic ratios that were confirmed in MCECs as well as in HCECs (Table 2). The protein expression of CD73, which was used as a representative marker of fibroblastic cells, was not observed in normal phenotype MCECs, while it was observed at the cell membrane in fibroblastic MCECs (Fig. 2B). On the

**TABLE 2.** Selected Markers of Nonfibroblastic and Fibroblastic CECs

Nonfibroblastic Phenotype	Fibroblastic Phenotype
CD98	CD9
CD166	CD44
CD340	CD49e
	CD73

other hand, CD166, which was used as a representative marker of normal cells, was observed at the cell membrane of nonfibroblastic MCECs, but not in fibroblastic MCECs. The PCR data also indicated that *CD73* was strongly expressed at the mRNA level in fibroblastic cells, but not in normal cells, while *CD166* was expressed in normal cells, but to a lesser extent in fibroblastic cells (Fig. 2C).

### CD73 Marks Fibroblastic MCECs With the Loss of Functional Phenotype via Epithelial Mesenchymal Transformation

Our goal was to detect possible contamination with vulnerable fibroblastic transformed cells, so we further investigated the reliability of using CD73 as a potential fibroblastic marker, since CD73 reportedly is involved in lung and liver fibrosis.<sup>24,25</sup> Experiments were conducted to determine whether fibroblastic cells could be detected by CD73 in a mixture of normal and fibroblastic cells by mixing nonfibroblastic MCECs and fibroblastic MCECs at 1:1 ratio (Fig. 3A) and then sorting out the CD73-negative and -positive cells (Fig. 3B). After culturing, the CD73-negative sorted MCECs exhibited a normal hexagonal morphology, whereas the CD73-positive MCECs exhibited fibroblastic morphology (Fig. 3C). The PCR analysis showed that CD73-negative MCECs did not express *CD73*, while CD73-positive MCECs expressed *CD73* at the mRNA level (Fig. 3D). A nonfibroblastic marker, *CD166*, was expressed in the CD73-negative MCECs, but *CD166* was expressed at a lower rate in the CD73-positive cells (Fig. 3D). The CD73-positive cells also expressed higher levels of *COL1A1*, an extracellular matrix

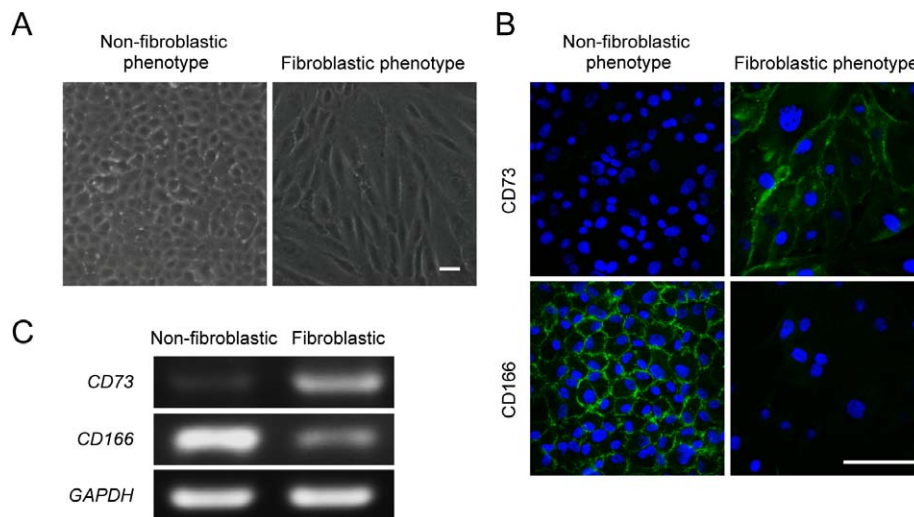


**FIGURE 2.** Expression of CD73 and CD166 in nonfibroblastic and fibroblastic MCECs. (A) The image on the *left* shows the MCECs of normal phenotype, while the image on the *right* shows MCECs of fibroblastic phenotype. Scale bar: 100  $\mu$ m. (B) The MCECs of nonfibroblastic and fibroblastic phenotypes were immunostained with the antibodies against CD73 and CD166. The fibroblastic phenotype cells expressed CD73 at the cell membrane, while no expression was observed in cells of normal phenotype. The CD166 was expressed at the cell membrane of normal phenotype cells, while it was very weakly stained in fibroblastic phenotype cells. Scale bar: 100  $\mu$ m. (C) The mRNA levels of *CD73* and *CD166* were evaluated using PCR. Gene *CD73* was expressed at higher levels in fibroblastic MCECs than in normal MCECs. On the other hand, *CD166* was expressed at higher levels in normal MCECs than in fibroblastic MCECs.

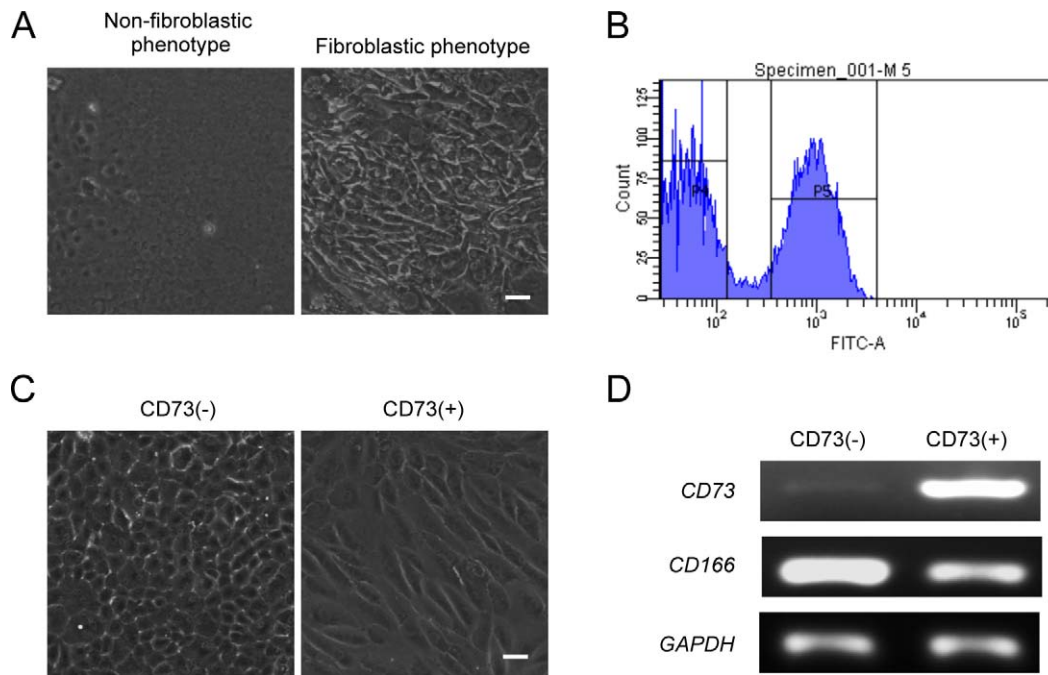


**FIGURE 3.** Cell sorting of MCECs by CD73. (A, B) Cultured MCECs exhibiting nonfibroblastic and fibroblastic phenotypes were harvested from the culture plate and mixed at 1:1 ratio. Mixed cells were stained for CD73 and were sorted by flow cytometry. Two peaks, CD73-positive and -negative, were observed. *Scale bar*: 100  $\mu$ m. (C) The MCECs were sorted according to the expression level of CD73 and were cultured to reach confluence. The CD73-negative cells had a hexagonal normal morphology, while CD73-positive cells had a fibroblastic morphology. *Scale bar*: 100  $\mu$ m. (D) The mRNA expression levels of *CD73* and *CD166* in sorted CD73-negative and -positive cells evaluated by PCR. The CD73-positive sorted cells expressed *CD73* at the mRNA level, while CD73-negative sorted cells expressed almost no *CD73*. On the other hand, *CD166* mRNA was expressed at a higher level in CD73-negative sorted cells than in CD73-positive sorted cells. These experiments were performed in triplicate.

protein produced under pathologic conditions by the corneal endothelium (Fig. 4A).<sup>26,27</sup> On the other hand, the CD73-positive cells showed a much lower expression of *COL4A1* and *COL8A1*, which normally are produced by the corneal endothelium (Fig. 4A). The CD73-positive cells also expressed higher levels of genes associated with induction of the epithelial mesenchymal transformation (EMT), such as *SNAI1*, *SNAI2*, and *ZEB1* (Fig. 4B). Staining for endothelial characteristics revealed that the staining pattern of ZO-1 and Na<sup>+</sup>/K<sup>+</sup>-ATPase at the plasma membrane was well preserved in CD73-negative MCECs, whereas the CD73-positive MCECs lost the characteristic staining profile of ZO-1 and Na<sup>+</sup>/K<sup>+</sup>-ATPase at the plasma membrane (Fig. 4C). The data for immunofluorescence staining were supported by mRNA expression data for *ZO1*, *ATP1A1*, and *CDH2*, which were expressed in CD73-negative MCECs, but showed low expression in CD73-positive MCECs (Fig. 4D).

### CD73 as a Cell Surface Marker for Fibroblastic HCECs

We also investigated whether CD73 could be used to detect the fibroblastic forms of human as well as monkey CECs. The primary cultured HCECs tended to undergo fibroblastic changes when passed through a cell strainer for flow cytometry, so we established immortalized nonfibroblastic and fibroblastic HCECs cell lines (Fig. 5A). The same types of experiments performed with MCECs were repeated with immortalized HCECs and cells expressing or not expressing CD73 were cultured (Fig. 5B). Flow cytometry analysis demonstrated that the purity of CD73-negative sorted immortalized HCECs was 97.6% (Fig. 5C). The CD73-negative immortalized HCECs again exhibited a normal hexagonal, contact-inhibited morphology, while CD73-positive immortalized HCECs exhibited a fibroblastic, stratified morphology (Fig. 5D).

Immunostaining showed that CD73 was expressed in the CD73-positive sorted immortalized HCECs, but not in CD73-negative sorted immortalized HCECs (even after further cultivation, Fig. 5E). The ZO-1 and Na<sup>+</sup>/K<sup>+</sup>-ATPase were functionally expressed at the plasma membrane in CD73-negative immortalized HCECs, while CD73-positive immortalized HCECs lost this normal expression of ZO-1 and Na<sup>+</sup>/K<sup>+</sup>-ATPase (Fig. 5E). The CD73-positive sorted immortalized HCECs expressed higher CD73 at the mRNA level than CD73-negative sorted immortalized HCECs (Fig. 5F).

Quantitative PCR analysis showed that expression of *ZO1* and *ATP1A1* was significantly reduced in CD73-positive cells compared to CD73-negative cells (Fig. 5G). On the other hand, expression of *FNI* was higher in CD73-positive cells than in CD73-negative cells (Fig. 5G).

Quantitative PCR analysis showed that expression of *ZO1* and *ATP1A1* was significantly reduced in CD73-positive cells compared to CD73-negative cells (Fig. 5G). On the other hand, expression of *FNI* was higher in CD73-positive cells than in CD73-negative cells (Fig. 5G).

### DISCUSSION

Extensive progress recently has raised the possibility of new therapeutic modalities based on tissue engineering techniques for various diseases.<sup>28,29</sup> However, although the FDA regulates interstate commerce in human cells and tissue-based products (HCT/Ps),<sup>30</sup> and although other countries also have similar systems,<sup>31</sup> the current regulatory frameworks are not presently viewed as providing sufficient coverage of innovative tissue engineering therapies.<sup>32</sup> In the present study, we investigated biological markers of HCECs for quality control with a view to clinical settings where cell characterization could be ensured. The Na<sup>+</sup>/K<sup>+</sup>-ATPase and ZO-1 investigated here are used frequently for research purposes, as coexpression of these proteins is recognized as identifying cells that possess pump

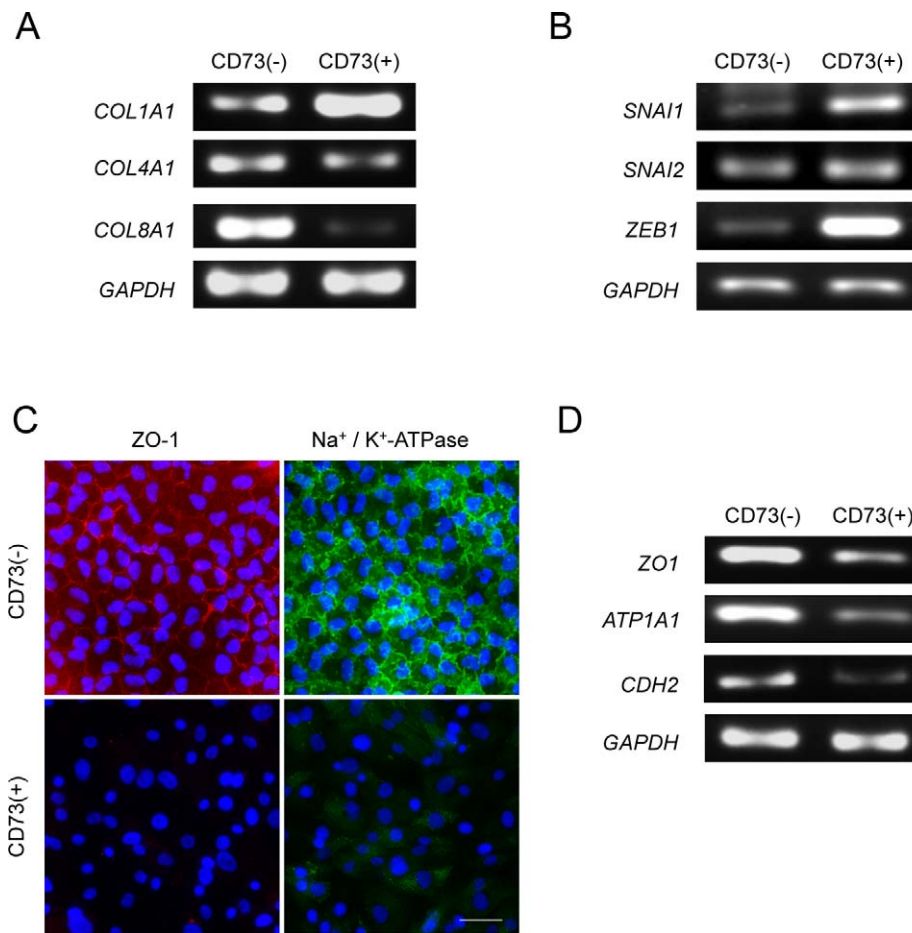


**FIGURE 4.** Functional analysis of CD73-positive MCECs. **(A)** Expressions of *COL1A1* (pathologic collagen of corneal endothelium), *COL4A1* (normal collagen), and *COL8A1* (normal collagen) in CD73-negative and -positive sorted cells were evaluated using PCR. Greater expression of *COL1A1* was seen in CD73-positive cells than in CD73-negative cells. Greater expression of *COL4A1* and *COL8A1* was found in CD73-negative sorted cells than in CD73-positive cells. **(B)** Expression of EMT inducer genes (*SNAI1*, *SNAI2*, and *ZEB1*) was evaluated by PCR. The CD73-positive sorted cells showed greater expression of *SNAI1*, *SNAI2*, and *ZEB1* when compared to CD73-negative cells. **(C)** Immunofluorescence staining of CD73-negative or -positive sorted cells by ZO-1 and Na<sup>+</sup>/K<sup>+</sup>-ATPase. Both ZO-1 and Na<sup>+</sup>/K<sup>+</sup>-ATPase were stained at the plasma membrane of CD73-negative cells. However, their expression was disrupted and decreased in CD73-positive cells. Scale bar: 50 μm. **(D)** Expression levels of *ZO1*, *ATP1A1*, and *CDH2* were evaluated using PCR. The CD73-negative cells expressed *ZO1*, *ATP1A1*, and *CDH2* at the mRNA level, while their expression was decreased in CD73-positive cells. These experiments were performed in triplicate.

and barrier functional activity.<sup>33,34</sup> However, these proteins are not specific to corneal endothelium and are expressed in other organs, such as the heart, kidneys, and brain.<sup>35-38</sup> The genes that are known to have a role in corneal endothelium, such as *SLC4A* (Na, HCO<sub>3</sub> co-transporter), *COL4A2* (type IV collagen), *COL8A2* (type VIII collagen), and *CDH2* (N-cadherin), also have been used as markers.<sup>39</sup> However, no single specific gene was identified as an HCEC marker,<sup>40</sup> even though gene expression profiles were reported in donor corneal endothelium.<sup>41,42</sup>

Recently, Glypican-4 and CD200 were proposed as HCEC markers to distinguish HCECs from corneal stromal fibroblasts, based on RNA sequencing and immunofluorescence staining.<sup>43</sup> However, the practical problem of HCEC culture is the potential contamination with vulnerable transformed HCECs,<sup>21</sup> so the purity of the cultured HCECs destined for clinical use must first be ensured. The lack of a specific marker led us to screen surface antigens that could be used to identify whether cultured cells retain their functional phenotype or have undergone fibroblastic changes. Further studies are required to determine which marker or combination of markers will be

most appropriate for quality control, but assessment of markers using flow cytometry will provide us with a quantitative threshold by which to ensure the functional characteristics for clinical application.

The results of the current study also pointed to the novel possibility of an in vitro cell expansion protocol, whereby purified HCECs can be separated from a general culture cell population possibly contaminated with transformed HCECs simply by using the positive and negative cell selection that is readily accomplished by FACS. Recent developments have enabled the inhibition of fibroblastic changes and greater success rates for cell culture,<sup>21</sup> but a cell selection technique still would be anticipated to ultimately circumvent potential contamination by fibroblastic cells.<sup>43</sup> Peh GS et al.<sup>44</sup> reported the separation of prefluorescein-labeled corneal stromal fibroblasts from a mixture of fibroblasts and HCECs by magnetic affinity cell separation (MACS) and suggested that this type of selection strategy would be useful for depleting the cultures of contaminating cells. To the best of our knowledge, ours is the first report showing this depletion of fibroblastic cells and purification of normal phenotype CECs from a mixed

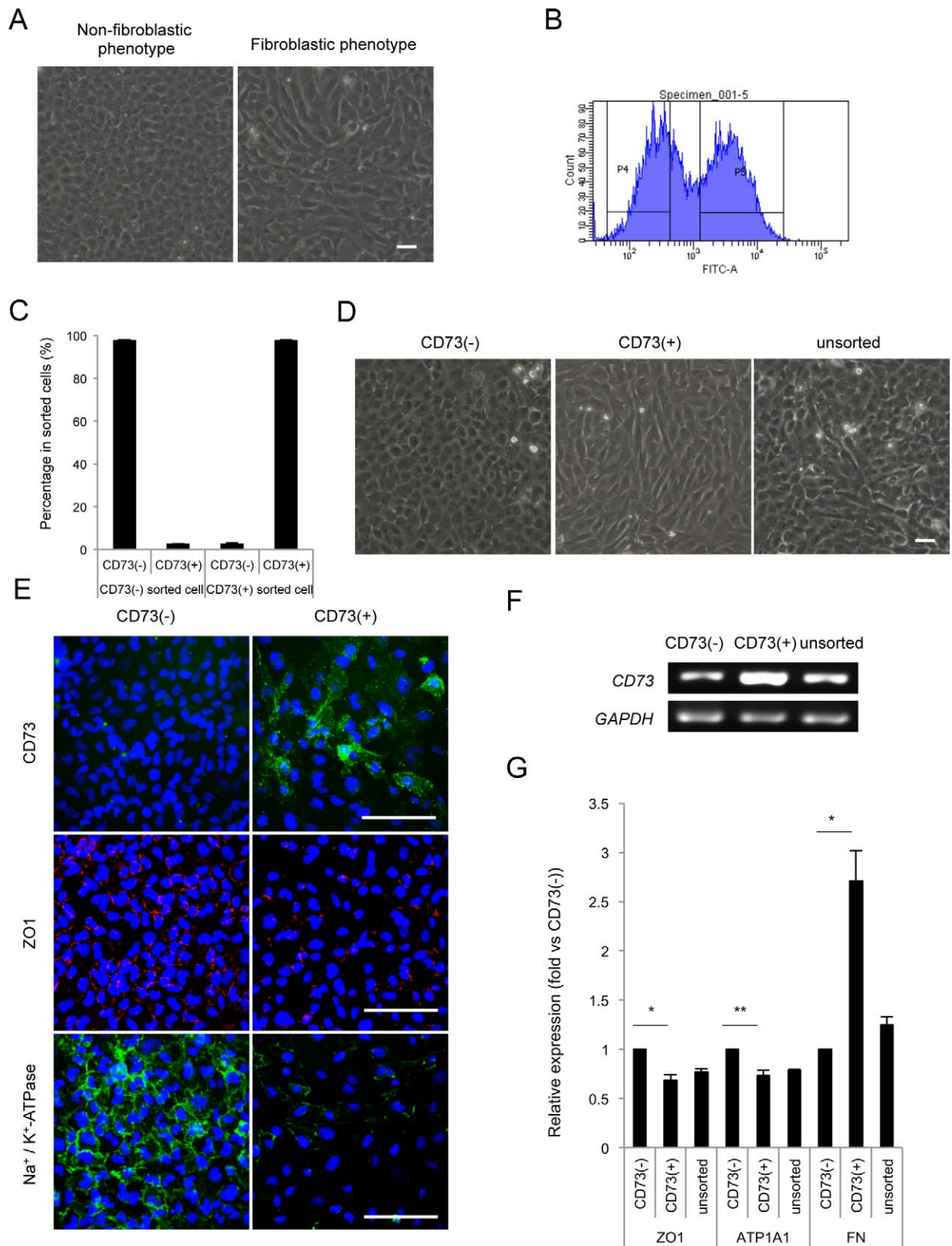


**FIGURE 5.** Cell sorting of immortalized HCECs and functional analysis of CD73-positive immortalized HCECs. (A) Normal hexagonal contact-inhibited phenotype HCECs and fibroblastic HCECs were immortalized using SV40 and hTERT to establish cell lines. (B) Immortalized normal HCECs and fibroblastic HCECs were harvested from culture plates and mixed. The CD73-negative and -positive cells then were sorted by flow cytometry. (C) The CD73-negative and -positive immortalized HCECs were sorted and CD73 expression was analyzed using flow cytometry. A total of 96.7% of CD73-negative sorted cells expressed CD73, while 97.6% of CD73-positive sorted cells did not express CD73. (D) The CD73-negative and -positive sorted immortalized HCECs were seeded and cultured until confluent. The CD73-negative cells showed hexagonal morphology, while CD73 (+) and unsorted control cells showed fibroblastic morphology. (E) Immunofluorescence staining of CD73, ZO-1, and Na<sup>+</sup>/K<sup>+</sup>-ATPase. The

CD73 staining was confirmed in CD73-positive sorted cells, while it was not stained in CD73-negative sorted cells. The CD73-negative cells expressed ZO-1 and Na<sup>+</sup>/K<sup>+</sup>-ATPase at the plasma membrane, while their expression was disrupted in CD73-positive cells. *Scale bar*: 100 μm. (F) Expression of *CD73* was assessed using PCR. The CD73-positive cells expressed higher levels of *CD73* mRNA than did the CD73-negative cells. (G) Expression of *ZO1*, *ATP1A1*, and *FNI* was assessed by quantitative PCR. The CD73-positive cells expressed less *ZO1* and *ATP1A1*, while expression of *FNI* was higher than in CD73-negative cells. \**P* < 0.01, \*\**P* < 0.05.

cell population using FACS. Although we successfully separated fibroblastic cells from the immortalized HCEC-population by FACS, primary cultured HCECs tended to exhibit fibroblastic changes after cell sorting by our current protocol, due to complete cell dissociation for FACS (data not shown). Thus, the details of this selection procedure, especially for human cells, should be optimized; for example, through the use of antifibroblastic molecule during cell dissociation<sup>21</sup> and the separation by MACS rather than FACS.<sup>44</sup> These results suggest that the depletion of fibroblastic cells based on cell surface antigens should be explored further to isolate a purified cell population for clinical use.

We considered that detection of fibroblastic cell contamination would be possible if we could discover a marker for fibroblastic HCECs. Indeed, CD73 enabled the detection of fibroblastic cells, and further separation of normal and fibroblastic cells. The CD73 (ecto-5'-nucleotidase) is membrane-bound glycoprotein that metabolizes adenosine 5'-monophosphate (AMP) to adenosine.<sup>45</sup> Expression of CD73 is observed in a variety of cell types and regulates various physiological phenomena, such as ion and fluid transport, barrier function, adaptation to hypoxia, and inflammation.<sup>45</sup> Little is known regarding the involvement of CD73 in fibroblastic transformation, but this glycoprotein has an important role in bleomycin-induced lung injury<sup>24</sup> and hepatic fibrosis<sup>25</sup> through the conversion of AMP to adenosine. In the corneal endothelium, we showed that EMT inducer genes, such as *SNAIL1*, *SNAIL2*, and *ZEB1*, were activated in CD73-positive cells,<sup>21</sup> which suggests that the EMT might be involved in the elevated expression of CD73.

In conclusion, we demonstrated that CD98, CD166, and CD340 could serve as markers of the nonfibroblastic phenotype of HCECs, and that CD9, CD44, CD49e, and CD73 could serve as markers of the fibroblastic phenotype of these cells. These markers could be used for quality control to characterize the cellular phenotype used in therapies based on tissue engineering, though the threshold for clinical use should be explored further. Further, if positive and negative cell selection proves applicable to clinical settings, cell sorting based on these cell surface markers will provide a novel strategy for purifying functional cells.

### Acknowledgments

The authors thank Satoshi Kawasaki, Kenta Yamasaki, Kazuko Asada, Munetoyo Toda, and Yuji Sakamoto for their valuable assistance with the experiments.

Disclosure: N. Okumura, P; H. Hirano, P; R. Numata, None; M. Nakahara, None; M. Ueno, P; J. Hamuro, None; S. Kinoshita, P; N. Koizumi, P

### References

- Bourne WM. Clinical estimation of corneal endothelial pump function. *Trans Am Ophthalmol Soc*. 1998;96:229-239, discussion 239-242.
- Joyce NC. Proliferative capacity of the corneal endothelium. *Prog Retin Eye Res*. 2003;22:359-389.
- Joyce NC. Cell cycle status in human corneal endothelium. *Exp Eye Res*. 2005;81:629-638.
- Koizumi N, Suzuki T, Uno T, et al. Cytomegalovirus as an etiologic factor in corneal endotheliitis. *Ophthalmology*. 2008;115:292-297.
- Tan DT, Dart JK, Holland EJ, Kinoshita S. Corneal transplantation. *Lancet*. 2012;379:1749-1761.
- Eye Bank Association of America. *Eye Banking Statistical Report*. Washington, DC: Eye Bank Association of America; 2012.
- Lee JA, Djalilian AR, Riaz KM, et al. Clinical and histopathologic features of failed Descemet stripping automated endothelial keratoplasty grafts. *Cornea*. 2009;28:530-535.
- Koizumi N, Okumura N, Kinoshita S. Development of new therapeutic modalities for corneal endothelial disease focused on the proliferation of corneal endothelial cells using animal models. *Exp Eye Res*. 2012;95:60-67.
- Mimura T, Yamagami S, Yokoo S, et al. Cultured human corneal endothelial cell transplantation with a collagen sheet in a rabbit model. *Invest Ophthalmol Vis Sci*. 2004;45:2992-2997.
- Ishino Y, Sano Y, Nakamura T, et al. Amniotic membrane as a carrier for cultivated human corneal endothelial cell transplantation. *Invest Ophthalmol Vis Sci*. 2004;45:800-806.
- Sumide T, Nishida K, Yamato M, et al. Functional human corneal endothelial cell sheets harvested from temperature-responsive culture surfaces. *FASEB J*. 2006;20:392-394.
- Koizumi N, Sakamoto Y, Okumura N, et al. Cultivated corneal endothelial cell sheet transplantation in a primate model. *Invest Ophthalmol Vis Sci*. 2007;48:4519-4526.
- Mimura T, Shimomura N, Usui T, et al. Magnetic attraction of iron-endocytosed corneal endothelial cells to Descemet's membrane. *Exp Eye Res*. 2003;76:745-751.
- Mimura T, Yokoo S, Araie M, Amano S, Yamagami S. Treatment of rabbit bullous keratopathy with precursors derived from cultured human corneal endothelium. *Invest Ophthalmol Vis Sci*. 2005;46:3637-3644.
- Patel SV, Bachman LA, Hann CR, Bahler CK, Fautsch MP. Human corneal endothelial cell transplantation in a human ex vivo model. *Invest Ophthalmol Vis Sci*. 2009;50:2123-2131.
- Okumura N, Koizumi N, Ueno M, et al. ROCK inhibitor converts corneal endothelial cells into a phenotype capable of regenerating in vivo endothelial tissue. *Am J Pathol*. 2012;181:268-277.
- Okumura N, Ueno M, Koizumi N, et al. Enhancement on primate corneal endothelial cell survival in vitro by a ROCK inhibitor. *Invest Ophthalmol Vis Sci*. 2009;50:3680-3687.
- Peh GS, Toh KP, Wu FY, Tan DT, Mehta JS. Cultivation of human corneal endothelial cells isolated from paired donor corneas. *PLoS One*. 2011;6:e28310.
- Shima N, Kimoto M, Yamaguchi M, Yamagami S. Increased proliferation and replicative lifespan of isolated human corneal endothelial cells with L-ascorbic acid 2-phosphate. *Invest Ophthalmol Vis Sci*. 2011;52:8711-8717.
- Nakahara M, Okumura N, Kay EP, et al. Corneal endothelial expansion promoted by human bone marrow mesenchymal stem cell-derived conditioned medium. *PLoS One*. 2013;8:e69009.
- Okumura N, Kay EP, Nakahara M, Hamuro J, Kinoshita S, Koizumi N. Inhibition of TGF-beta signaling enables human corneal endothelial cell expansion in vitro for use in regenerative medicine. *PLoS One*. 2013;8:e58000.



22. Okumura N, Koizumi N, Kay EP, et al. The ROCK inhibitor eye drop accelerates corneal endothelium wound healing. *Invest Ophthalmol Vis Sci.* 2013;54:2493-2502.
23. Peh GS, Beuerman RW, Colman A, Tan DT, Mehta JS. Human corneal endothelial cell expansion for corneal endothelium transplantation: an overview. *Transplantation.* 2011;91:811-819.
24. Volmer JB, Thompson LF, Blackburn MR. Ecto-5'-nucleotidase (CD73)-mediated adenosine production is tissue protective in a model of bleomycin-induced lung injury. *J Immunol.* 2006;176:4449-4458.
25. Fausther M, Sheung N, Saiman Y, Bansal MB, Dranoff JA. Activated hepatic stellate cells upregulate transcription of ecto-5'-nucleotidase/CD73 via specific SP1 and SMAD promoter elements. *Am J Physiol Gastrointest Liver Physiol.* 2012;303:G904-G914.
26. Kawaguchi R, Saika S, Wakayama M, Ooshima A, Ohnishi Y, Yabe H. Extracellular matrix components in a case of retrocorneal membrane associated with syphilitic interstitial keratitis. *Cornea.* 2001;20:100-103.
27. Weller JM, Zenkel M, Schlotzer-Schrehardt U, Bachmann BO, Tourtas T, Kruse FE. Extracellular matrix alterations in late-onset Fuchs' corneal dystrophy. *Invest Ophthalmol Vis Sci.* 2014;55:3700-3708.
28. Okano H, Nakamura M, Yoshida K, et al. Steps toward safe cell therapy using induced pluripotent stem cells. *Circ Res.* 2013;112:523-533.
29. Tabar V, Studer L. Pluripotent stem cells in regenerative medicine: challenges and recent progress. *Nat Rev Genet.* 2014;15:82-92.
30. Lysaght T, Campbell AV. Regulating autologous adult stem cells: the FDA steps up. *Cell Stem Cell.* 2011;9:393-396.
31. Sipp D. Hope alone is not an outcome: why regulations makes sense for the global stem cell industry. *Am J Bioeth.* 2010;10:33-34.
32. Hyun I. Allowing innovative stem cell-based therapies outside of clinical trials: ethical and policy challenges. *J Law Med Ethics.* 2010;38:277-285.
33. Barry PA, Petroll WM, Andrews PM, Cavanagh HD, Jester JV. The spatial organization of corneal endothelial cytoskeletal proteins and their relationship to the apical junctional complex. *Invest Ophthalmol Vis Sci.* 1995;36:1115-1124.
34. Sugrue SP, Zieske JD. ZO1 in corneal epithelium: association to the zonula occludens and adherens junctions. *Exp Eye Res.* 1997;64:11-20.
35. Fanning AS, Anderson JM. Zonula occludens-1 and -2 are cytosolic scaffolds that regulate the assembly of cellular junctions. *Ann N Y Acad Sci.* 2009;1165:113-120.
36. Sune G, Sarro E, Puigmule M, et al. Cyclophilin B interacts with sodium-potassium ATPase and is required for pump activity in proximal tubule cells of the kidney. *PLoS One.* 2010;5:e13930.
37. Corti C, Xuereb JH, Crepaldi L, Corsi M, Michielin F, Ferraguti F. Altered levels of glutamatergic receptors and Na<sup>+</sup>/K<sup>+</sup> ATPase- $\alpha$ 1 in the prefrontal cortex of subjects with schizophrenia. *Schizophr Res.* 2011;128:7-14.
38. Sanchez C, Corrias A, Bueno-Orovio A, et al. The Na<sup>+</sup>/K<sup>+</sup> pump is an important modulator of refractoriness and rotor dynamics in human atrial tissue. *Am J Physiol Heart Circ Physiol.* 2012;302:H1146-1159.
39. Hatou S, Yoshida S, Higa K, et al. Functional corneal endothelium derived from corneal stroma stem cells of neural crest origin by retinoic acid and Wnt/beta-catenin signaling. *Stem Cells Dev.* 2013;22:828-839.
40. Chng Z, Peh GS, Herath WB, et al. High throughput gene expression analysis identifies reliable expression markers of human corneal endothelial cells. *PLoS One.* 2013;8:e67546.
41. Sakai R, Kinouchi T, Kawamoto S, et al. Construction of human corneal endothelial cDNA library and identification of novel active genes. *Invest Ophthalmol Vis Sci.* 2002;43:1749-1756.
42. Gottsch JD, Seitzman GD, Margulies EH, et al. Gene expression in donor corneal endothelium. *Arch Ophthalmol.* 2003;121:252-258.
43. Cheong YK, Ngho ZX, Peh GS, et al. Identification of cell surface markers glypican-4 and CD200 that differentiate human corneal endothelium from stromal fibroblasts. *Invest Ophthalmol Vis Sci.* 2013;54:4538-4547.
44. Peh GS, Lee MX, Wu FY, Toh KP, Balchousur D, Mehta JS. Optimization of human corneal endothelial cells for culture: the removal of corneal stromal fibroblast contamination using magnetic cell separation. *Int J Biomater.* 2012;2012:601302.
45. Colgan SP, Eltzschig HK, Eckle T, Thompson LF. Physiological roles for ecto-5'-nucleotidase (CD73). *Purinergic Signal.* 2006;2:351-360.